Atmos. Chem. Phys. Discuss., 12, 30371–30407, 2012
www.atmos-chem-phys-discuss.net/12/30371/2012/
doi:10.5194/acpd-12-30371-2012

Atmospheric Chemistry and Physics Discussions

This discussion paper is/has been under review for the journal Atmospheric Chemistry and Physics (ACP). Please refer to the corresponding final paper in ACP if available.

Influence of the sunspot cycle on the Northern Hemisphere wintertime circulation from long upper-air data sets

Y. Brugnara[1,2], S. Brönnimann[1,2], J. Luterbacher[3], and E. Rozanov[4,5]

[1]Institute of Geography, University of Bern, Bern, Switzerland
[2]Oeschger Centre for Climate Change Research, Bern, Switzerland
[3]Department of Geography, Climatology, Climate Dynamics and Climate Change, Justus-Liebig University of Giessen, Giessen, Germany
[4]Physikalisch-Meteorologisches Observatorium Davos, World Radiation Center, Davos, Switzerland
[5]Institute for Atmospheric and Climate Science ETH, Zurich, Switzerland

Received: 15 October 2012 – Accepted: 18 November 2012 – Published: 23 November 2012

Correspondence to: S. Brönnimann (stefan.broennimann@giub.unibe.ch)

Published by Copernicus Publications on behalf of the European Geosciences Union.

Abstract

Here we present a study of the 11-yr sunspot cycle's imprint in the Northern Hemisphere atmospheric circulation, using three recently developed gridded upper-air data sets which extend back to the early twentieth century. We find a robust response of the tropospheric late-wintertime circulation to the sunspot cycle, independent from the data set. This response is particularly significant over Europe, but results show that it is not directly related to a North Atlantic Oscillation modulation; instead, it reveals a significant connection to the more meridional Eurasian pattern. The magnitude of mean seasonal temperature changes over the European land areas locally exceeds 1 K in the lower troposphere over a sunspot cycle.

We also analyse surface data to address the question whether the solar signal over Europe is temporally stable for a longer 250 yr period. The results increase our confidence on the existence of an influence of the 11-yr cycle on the European climate, although the signal is much weaker in the first half of the period compared to the second half. The last solar minimum (2005 to 2010), which was not included in our analysis, shows anomalies that are consistent with our statistical results for earlier solar minima.

1 Introduction

For more than two centuries scientists have been speculating on a possible influence of the solar output variability on Earth's climate and atmospheric dynamics (Gray et al., 2010 for a review; Lockwood, 2012). Research in this field has progressed significantly during the last decade, mainly due to the use of global circulation models coupled with ocean dynamics and chemical processes in the stratosphere (see Gray et al., 2010 for a review). In particular, a large part of the research focused on the decadal variations of total and spectral solar irradiance, namely the 11-yr cycle. This cycle determines a change in the Total Solar Irradiance (TSI) at the top of the Earth's atmosphere of about 0.1 % (i.e. of the order of 1 $\mathrm{W\,m^{-2}}$), but a much larger change in the ultraviolet (UV) part

Discussion Paper | Discussion Paper | Discussion Paper | Discussion Paper |

ACPD

12, 30371–30407, 2012

Influence of the sunspot cycle on the Northern Hemisphere wintertime circulation

Y. Brugnara et al.

of the spectrum, up to 3 % according to recent measurements by the SORCE satellite (Harder et al., 2009). It also modulates the strength of galactic cosmic rays reaching the Earth and geomagnetic activity (e.g. Tinsley and Yu, 2004). Each of these changes could have an impact on climate (see Gray et al., 2010 for a review). However, the relatively short period covered by observations still represents a bottleneck for a reliable quantification of this impact, especially for the troposphere. A wide spatial coverage of the atmosphere is needed, both on horizontal and vertical scale, in order to allow the validation of model simulations and to study the physical mechanisms involved. Until recently, the only data sets fulfilling this requisite were reanalyses that cover not more than five solar cycles, or even less if homogeneity issues are taken into account. In particular, ERA-40 (Uppala et al., 2005) and NCEP/NCAR (Kalnay et al., 1996; Kistler et al., 2001) reanalyses are widely used. Frame and Gray (2010) analysed the statistical relationships between the solar radio flux at 10.7 cm and zonally-averaged temperature and zonal wind in ERA-40, but they were forced to use only data from 1978 onward due to the lack of stratospheric observations in the earlier period; moreover, data after 2002 were taken from another reanalysis product. They found significant correlations in the tropical stratosphere throughout the year, while results in the troposphere were less clear. Haigh (2003) did a similar analysis for temperature in NCEP/NCAR over the period 1979–2001, finding a stronger correlation in the subtropical troposphere. Gleisner et al. (2005) tried to compare the two reanalyses over the period 1958–2001 and concluded that substantial discrepancies between the two data sets in the 1970s and the 1980s cause large differences in the correlations with the solar flux in the troposphere, particularly in the tropics and in the Southern Hemisphere; in general the correlations are much higher in NCEP/NCAR. Other inhomogeneities in the reanalyses, potentially affecting the reliability of the statistical relations with solar variability, were pointed out by other authors (e.g. Bengtsson et al., 2004; Kinter et al., 2004).

Results from surface data, which are available for longer periods and are normally more reliable, suggest at least the existence of a solar influence. Previous studies found a significant solar influence on the wintertime sea level pressure field of the Northern

ACPD
12, 30371–30407, 2012

Hemisphere (e.g. Kodera, 2003; Van Loon et al., 2007; Roy and Haigh, 2010, 2011; Woollings et al., 2010; Bal et al., 2011; Ineson et al., 2011; Martin-Puertas et al., 2012). It is important to note that the signals often differ largely in strength and significance among the various studies, because they are based on different data sets, periods and statistical methods. However two common features are the weakening (strengthening) of the Aleutian low and the strengthening (weakening) of the Icelandic low during maxima (minima) of solar activity, with consequent changes in wind and temperature patterns over North America and Europe.

Other studies focused on regions where upper-air data are reliable for long periods, typically in the mid-latitudes of the Northern Hemisphere. For instance, Brönnimann et al. (2007a) found a significant solar influence in the zonal mean of geopotential height in the upper troposphere over the period 1922–2003, when averaged over a latitudinal band spanning from 30° N to 60° N.

The present paper aims at a more detailed and reliable description of the statistical relations between the tropospheric wintertime circulation in the Northern Hemisphere and the 11-yr solar cycle over the last century, using state-of-the-art observational data sets. Long statistical reconstructions of surface and upper-air parameters have been created in recent years, pushed by big efforts made in the recovery and digitizing of old data. Furthermore, a 140-yr long reanalysis has been developed based on surface data only (Compo et al., 2011), yet demonstrating good performances for the Northern Hemisphere even in the upper troposphere for some variables (e.g. geopotential height). Our purpose is then to exploit these new data sets for a better description of the decadal variability driven by the Sun, in particular in the wintertime troposphere over North America and Europe, i.e. where the largest amount of upper-air data is available. For these regions we have the possibility to use data from the first half of the 20th century, which is fundamental to address the stability of the solar signals. Measurements of the solar radio flux are available only from the 1950s, but periods of maxima and minima of the 11-yr cycle can still be detected from direct observations of sunspots, which are the most commonly used proxy for solar activity. In fact, the number of dark

ACPD
12, 30371–30407, 2012

spots on the Earth-directed face of the Sun has been observed for centuries and a reconstruction is available for the last 300 yr (for historical details refer to Eddy, 1976).

We use different, independently-developed data sets and different, complementary statistical approaches to improve the robustness of the analysis. The combination of these data sets and statistical methods provide a more reliable picture of solar induced tropospheric circulation changes than hitherto possible.

After a presentation of the data sets and the statistical methods used, we present first the results on long reconstructions of sea level pressure (SLP) for the Euro–Atlantic area, then we compare them to the results for upper-air reconstructions and reanalysis in the last century. Finally we discuss the coherency of the various results and describe a "solar pattern" which seems to be stable for more than 250 yr.

2 Data

2.1 SLP and atmospheric circulation indices

We use the monthly gridded SLP reconstruction for the North Atlantic–European (NAE) region (30° W to 40° E; 30° N to 70° N) from Luterbacher et al. (2002), which covers the period 1659–2002. The statistical reconstruction is based on a combination of early instrumental station series and documentary proxy evidence.

Furthermore, we consider also the monthly circulation indices reconstructed by Luterbacher et al. (1999, 2001) up to 1990. The indices are the North Atlantic Oscillation (NAO) and the Eurasian index (EU; Luterbacher et al., 1999); the former is the most prominent mode of variability in the Northern Hemisphere (Barnston and Livezey, 1987), the latter plays an important role in the variability of Eurasian climate, especially during wintertime (Schmutz and Wanner, 1998). We analyse two versions of the NAO index and two versions of the EU index. NAO1 is calculated from gridded values of SLP, while NAO2 is from station data. EU1 (EU2) is defined as the standardized, grid point based SLP difference between Great Britain and the Black Sea (Caspian Sea).

ACPD
12, 30371–30407, 2012

The reader is referred to Luterbacher et al. (1999) for further details on the definition of the indices.

2.2 Upper-air data sets

The main data sets are recently developed statistical reconstructions of global upper-air fields for temperature, wind and geopotential height: REC1 (Griesser et al., 2010) and REC2 (Brönnimann et al., 2012b). These gridded (2.5° × 2.5°) reconstructions are based on surface air temperature from the NASA-GISS station data set (Hansen et al., 1999), sea-level pressure data from HadSLP2 (Allan and Ansell, 2006) and upper-air observations from the Comprehensive Historical Upper-Air Network (CHUAN; Stickler et al., 2010). For REC1, three different reconstructions were performed: one for the Northern Hemisphere, one for the tropics and one for the Southern Hemisphere. Here we use the first one, which covers the latitudes from 15° N to 90° N. The lack of upper-air observations before the 1940s (Griesser et al., 2010) makes the tropical reconstruction not suitable for the purposes of this paper.

Data fields are available with monthly resolution at 6 levels (850, 700, 500, 300, 200, 100 hPa), except for the wind field in REC1 which is available only for the altitude of 3 km.

The main difference between the two data sets is related to the statistical approach. REC1 is based on the assumption of stationary large-scale patterns, thus it has the advantage of being a spatially complete data set with a long temporal coverage (1880–1957), but it is not suitable for detecting non-stationary teleconnections (Griesser et al., 2010). In REC2 each grid column is reconstructed independently using only predictors from a "cone of influence" around that grid column, with a minimum of 50 % information from upper-air data. REC2 has the disadvantage of an incomplete spatial coverage and a shorter length (1918–1957), but the approach assures that the reconstructed values are always close to observed upper-air data.

Both reconstructions are calibrated with the ERA-40 reanalysis, from which data for the period 1958–2002 were extracted. We then chose a period in which a minimum of

Discussion Paper | Discussion Paper | Discussion Paper | Discussion Paper |

ACPD

12, 30371–30407, 2012

Influence of the sunspot cycle on the Northern Hemisphere wintertime circulation

Y. Brugnara et al.

500 grid points are available in REC2, with the aim to find a good compromise between temporal length and spatial coverage. The evolution of the number of available grid points is shown by Fig. 1. A grid point is considered available for a certain period when it has a maximum of 5 missing years over that period (none of them can be the first year). These criteria led to 1927–2002 (7 solar cycles) as base period of the analysis. Most of the available grid points are over landmasses in the mid-latitudes of the Northern Hemisphere, covering a large part of North America and Europe; in addition, a few grid points are available in the Caribbean Sea.

Furthermore, we compare the statistical reconstructions with the Twentieth Century Reanalysis, hereafter 20CR (Compo et al., 2011). This reanalysis is based on sea-surface temperatures (SST) and SLP only, which means that it is almost independent from both REC1 and REC2 (SLP being the only common input, although with a different temporal resolution).

20CR is not affected by some common inhomogeneities of reanalysis products, such as the ones caused by the introduction of satellite-based measurements of upper-air temperature at the end of the 1970s. However, it is based on the version 2 of the Hadley Centre SST data set (HadSST2; Rayner et al., 2006), which has been shown to have a large inhomogeneity in the mid-1940s due to uncorrected instrumental biases in the ship-based measurements of water temperature (Thompson et al., 2008). The impact of this inhomogeneity on the upper-air fields of 20CR has not yet been evaluated in the published literature. 20CR also suffers from a large, time-varying bias in the temperature and wind in the Arctic (Brönnimann et al., 2012a).

3 Methods

We concentrate on the late-winter season (January to March, or JFM), when solar influence is expected to be at its peak in the troposphere. In fact, several studies suggested a propagation of the solar signal from the stratosphere to the troposphere during the

ACPD
12, 30371–30407, 2012

winter season (e.g. Shindell et al., 1999; Ineson et al., 2011), hence a signal in the troposphere is expected to appear only in late winter.

We use two different statistical methods: the difference of composites and the multiple linear regression (MLR). The former method is particularly useful to detect the influence of the 11-yr cycle, by looking for statistically significant differences between the mean fields during solar maxima and solar minima. Years with strong El Niño/La Niña (hereafter ENSO) episodes (as listed in Brönnimann et al., 2007b) or major volcanic eruptions are excluded from the analysis (we defined a winter to be volcanic when the average stratospheric optical depth of the Northern Hemisphere (30–90° N) from the reconstruction of Crowley et al. (2008) is greater than 0.05 in JFM minus 6 months, i.e. in the period from July to September of the previous year). The reason is the non-negligible influence of strong volcanic or ENSO episodes on the wintertime extra-tropical circulation (e.g. Moron and Plaut, 2003; Brönnimann et al., 2007b; Fischer et al., 2008; Graf and Zanchettin, 2012; Zanchettin et al., 2012a, b). Twenty-five volcanic winters were excluded according to our criterion since 1749; fourteen of them are in the nineteenth century, six of which in the 1810s. We can therefore exclude a large volcanic or ENSO bias in our results.

To discriminate between solar maxima and minima, we considered the upper (for maxima) and lower (for minima) terciles of the seasonal mean of the International Sunspot Number record ($R = 10\,N + n$, where N is the number of sunspot groups on the visible solar disk and n is the number of individual sunspots), downloaded from the Royal Observatory of Belgium's website (http://sidc.oma.be/sunspot-data/SIDCpub.php). Application of this approach for periods of steady increase of the solar activity (e.g. 1900–1950) is not straightforward, because some reconstructions (e.g. Shapiro et al., 2011) show long-term TSI trend which could lead to the fact that TSI for sunspot maximum around 1900 could be comparable or even lower than TSI for sunspot minimum around 1945. However, some other studies (e.g. Schrijver et al., 2011) conclude that the long term trend of the TSI does not exist, which justifies the application of R as a proxy for creating our composites. The sunspot number, plotted in Fig. 2, is

ACPD
12, 30371–30407, 2012

available with a monthly resolution starting from the year 1749, therefore we analyse the solar signal at the surface in the period 1749–2002 (1749–1990 for the circulation indices), which covers 23 solar cycles. This is also the period when the surface reconstructions are more reliable, since the first station pressure series become available in the mid-18th century (Luterbacher et al., 1999, 2001, 2002).

For the surface analysis we estimated the terciles of R from the whole period 1749–2002, for the upper-air analysis from the period 1927–2002 (because of the higher solar variability in that period); the thresholds are shown in Fig. 2. Other ways to define the composites, like using different thresholds for each cycle, did not influence remarkably our results. Furthermore we tried to use the open solar flux (Lockwood et al., 2009; Woollings et al., 2010) as a proxy instead of R, but also in this case the results did not change (not shown).

The significance of the difference for each grid point was calculated from a standard Student's t-test. Field significance was estimated by adapting the method proposed by Livezey and Chen (1983). We run a Monte Carlo simulation that consisted in replacing the years in the two composites with random years and calculating the number of grid points m with a significant difference (at 5 % level) for the random composites. The process was repeated 1000 times, leading to the null-distribution of m. The 95th percentile of the null-distribution represents our significance threshold m_{95} (i.e. the minimum m to be achieved in order to have a significant solar influence).

MLR can better separate the influence of solar activity from the influence of other known factors (e.g. ENSO, volcanoes), assuming that each predictor has a linear relationship with the predictand. The predictors used in the MLR are R representing solar activity, the Nino3.4 index (Rayner et al., 2003) representing ENSO, the Northern Hemisphere average of the stratospheric optical depth (Crowley et al., 2008) representing volcanic activity, the smoothed (10-yr running average) Atlantic Multi-decadal Oscillation Index (Enfield et al., 2001) representing oceanic low-frequency variability, and a linear trend. We applied a lead of 4 months to the ENSO predictor and of 6 months to the volcanic predictor (e.g. Brönnimann et al., 2007a; Lean and Rind, 2008) in order to

ACPD
12, 30371–30407, 2012

Title Page
Abstract Introduction
Conclusions References
Tables Figures
◀◀ ▶▶
◀ ▶
Back Close
Full Screen / Esc
Printer-friendly Version
Interactive Discussion

allow the propagation of the signals to high latitudes (the choice of the lead does not affect the results, not shown). The equation that describes our least squares regression model has the form:

$$y(\lambda,\phi,t) = c_0 + c_t(\lambda,\phi)\cdot t + c_R(\lambda,\phi)\cdot R(t) + c_{\mathrm{ENSO}}(\lambda,\phi)\cdot \mathrm{Nino3.4}(t) + c_{\mathrm{VOLC}}(\lambda,\phi)\cdot \mathrm{sod}(t) + c_{\mathrm{AMO}}(\lambda,\phi)\cdot \mathrm{AMO}(t) + \mathrm{res}(\lambda,\phi,t), \quad (1)$$

where λ is longitude, ϕ is latitude, t is time in years and res represents the residuals, i.e. the differences between observed and modelled data.

For the estimation of the uncertainty in the regression coefficients we took into account the autocorrelation of the residuals, adopting the same method described in Garny et al. (2007).

As we are mainly interested in the decadal signal, the difference of composites is the primary method adopted in this paper, while we use MLR to show that the choice of the method does not significantly influence the final results.

4 Solar signal at the surface

4.1 SLP field

The difference of solar maxima and minima composites for the late wintertime shows a negative solar signal in a wide area between Iceland and the British Islands (corresponding to 28 grid points, which is statistically significant since $m_{95} = 24$), where the pressure is more than 2 hPa lower in the solar maxima subset, indicating a strengthening of the Icelandic low (Fig. 3a). This result is in qualitative agreement with previous studies based on shorter data sets (Roy and Haigh, 2010; Woollings et al., 2010; Ineson et al., 2011), however our results indicate a more significant signal in the North Atlantic and a less strong response over North-Western Africa. Differences in the results might be also due to a different definition of the winter season and the use of different data sets.

ACPD
12, 30371–30407, 2012

In order to assess the stability and the robustness of the signal, we repeated the analysis using two sub-series of the SLP record spanning the first and the second half of the whole period (1749–1875 and 1876–2002, respectively). The respective composites differences are shown in Fig. 3b–c. The solar signal maintains its shape in the two sub-periods, although in the first period it is not statistically significant.

By looking separately at each single month (see Fig. S1 in the Supplement), we found that the signal is stable from January to March and it subsequently disappears in April, confirming that the choice of JFM for the analysis was justified.

4.2 NAO indices

The solar signal in the SLP and geopotential height fields over the NAE region has been often interpreted as a solar modulation of the NAO (e.g. Shindell et al., 2001; Boberg and Lundstedt, 2002, 2003; Kodera, 2003; Thejll et al., 2003; Woollings et al., 2010; Ineson et al., 2011). The differences between the maximum and minimum composites for the two versions of the NAO index for JFM over the period 1749–1990 are summarized in Table 1. Volcanic and ENSO years were excluded from the calculation adopting the same criteria used before, but we also provide the results for the unfiltered data sets for comparison. The NAO index is slightly higher (i.e. more positive) during solar maxima, but the difference does not reach the significance level of 5 % after a standard two-sided Student's t-test.

4.3 EU indices

Table 1 shows also the composite differences for the two EU indices. Contrary to NAO's case, we found a significant solar influence for both EU1 and EU2, even when disturbed years are not filtered out (however the significance of the differences decreases when volcanic and ENSO years are not removed). A scatter plot of EU1 against R is shown in Fig. 4; interestingly enough, during solar minima the EU1 index had strongly negative values only for volcanic or ENSO years.

5 Solar signal in the upper-air data

5.1 Geopotential height

A significant solar influence on the boreal extra-tropical geopotentials can be detected at all tropospheric levels. In Fig. 5 we show the composites difference for 300 hPa geopotential heights in the three considered data sets for the period 1927–2002. Figure 6 presents the same, but using the MLR. Results are very similar for the lower levels (not shown).

The three data sets agree quite well on the pattern of the solar signal in the upper troposphere, which appears as a tripole with negative centres over Iceland and North-Eastern Africa and a wide positive centre stretching from Western Mediterranean to Eastern Europe following a southwest-to-northeast axis. Another spot of significant negative differences is detectable over the west coast of North America. 20CR shows slightly stronger signals in the mid-latitudes, while the statistical reconstructions reveal a much stronger solar influence in the tropics. For the latter discrepancy we believe that the reconstructions are more reliable since they are based on real upper-air data, moreover the quality of 20CR is much lower in the tropics than in the mid-latitudes (Compo et al., 2011).

The MLR gives almost identical results at high latitudes, while in the tropics some remarkable differences in the magnitude of the signal are prevalent in the Gulf of Mexico (for REC2). Note that the values of the solar coefficient in Fig. 6 are scaled to represent a change of 100 units of the sunspot number and they are not directly comparable to the composites differences.

In general, the discrepancies in the solar signal that arise from the use of different data sets and different methods make our confidence in the results for tropical latitudes clearly lower.

5.2 Wind

The changes in the geopotential field imply changes in the atmospheric circulation, which can be observed in Figs. 7 and 8 for the u and v component of the 300 hPa wind respectively. Note that these variables are not available in REC1, therefore only REC2 and 20CR are shown.

The zonal flow is particularly affected at sub-tropical latitudes, where we find a clear weakening of the sub-tropical jet over North Africa during solar maxima. An important caveat for this claim is that we can rely only on 20CR, as REC2 does not cover the area of interest.

At solar maximum the zonal flow is enhanced over the southern part of the United States. In this case the two data sets do not agree very well, the signal is stronger and wider in REC2. The agreement is better for Western Europe, where another significant signal is found. 20CR indicates also a reduction of the wind speed between Iceland and Greenland; another smaller weakening is detectable over South-Western Canada, suggesting a southward shift of the polar jet.

A strong solar influence is present for the meridional component over Northern and Western Europe (Fig. 8). The significantly higher v during maxima actually represents a weaker meridional circulation, because in that area v is climatologically negative (i.e. southward). Figure 9 helps in the interpretation of this feature, showing how different the wind field appears over Europe depending on the phase of the solar cycle. During minima the air flow is substantially recurved to the south and north-westerlies dominate over much of Central Europe. This can be seen as a larger amplitude of the stationary planetary wave which characterises European climate (see e.g. Peixoto and Oort, 1992). In contrast with the results for the other variables, the solar signal does not reach the field significance threshold in REC2 for v, when considering all the grid points (it is however significant when considering Europe only). 20CR suggests a wave-like pattern of influence with most of the centres of action (Greenland, Eastern Mediterranean, Eastern Africa) outside of the area covered by REC2. Over North America the merid-

ACPD
12, 30371–30407, 2012

ional wind is not significantly affected, although a larger solar influence is present over the North-Eastern Pacific Ocean in 20CR.

For REC1, only the wind field at an altitude of 3 km is available. For the sake of completeness, we analysed this field too by comparing it with 700 hPa wind from the other two data sets (after 1957 the 3 km wind field has been linearly interpolated from ERA-40). The results are shown in Figs. S2 and S3 in the Supplement for u and v component, respectively. The agreement between the data sets is very good, the patterns in 20CR are also found in REC1. Another interesting result is the small dependence of the solar fingerprint from the choice of the level, at least in the troposphere (see Figs. 7 and 8 for comparison).

5.3 Temperature

Figure 10 shows the composites difference for temperature field at 300 hPa. Not surprisingly, the disagreement between the reconstructions and the reanalysis is more pronounced than for geopotential height or wind. The temperature field is not expected to be very reliable in 20CR, but also in the reconstructions its estimated uncertainty is high if compared to the other variables (Griesser et al., 2010; Brönnimann et al., 2012b).

The analyses for REC1 and REC2 exhibit a large area of positive temperature difference which goes from the Tropical Pacific to Southern Europe. 20CR, on the other side, shows a significant negative difference over North America and the North Atlantic. In both cases there is a higher meridional gradient during solar maxima, which is physically consistent with the stronger zonal winds that we observe in Fig. 7.

Even more remarkable is the impact in the lower troposphere. Here we observe a strong amplification of the solar imprint over Europe, with up to 1.5 K of difference between maximum and minimum at 850 hPa, while the solar signal almost disappears over North America (Fig. 11).

ACPD
12, 30371–30407, 2012

20CR results are much closer to the reconstructions for 850 hPa temperatures, although they seem to underestimate the solar signal over Eastern Europe (we recall that temperature on continents is entirely model-driven in 20CR).

5.4 Solar cycle 23

The solar cycle 23 that ended in 2010 was distinguished by an unusually long and deep minimum (Russell et al., 2010), which lies outside of the period analysed in this paper. It is interesting to look at the anomalies in the atmospheric circulation during the last minimum and to compare them with our results. Figure 12 shows the average anomalies for the winters (JFM) of 2005, 2006 and 2009 from 20CR (2007, 2008 and 2010 are not considered because they were influenced by strong ENSO episodes). Given the reduced number of years, the internal variability could in principle hide any solar influence even though the stronger source of variability (i.e. ENSO) was in large part removed. Nonetheless, the similarity with the results for 1927–2002 is striking for the Euro–Atlantic sector (note that the signals have the opposite sign because we are now considering a minimum).

6 Discussion and conclusions

Our results described a physically consistent picture of the sunspot cycle influence on the tropospheric circulation in the Northern Hemisphere. An increased (decreased) horizontal thermal gradient between low and high latitudes in late winter during solar maxima (minima) is accompanied by stronger (weaker) westerlies, in particular over Western Europe, and a smaller (bigger) amplitude of the stationary planetary wave.

The length of the analysed period, covering seven full sunspot cycles, allowed a more reliable statistical quantification of the solar signal, which can be easily affected by the noise of the natural variability on short timescales. A Monte Carlo test confirmed that

ACPD
12, 30371–30407, 2012

the solar influence over the analysed area is statistically significant for almost every level and every variable also when spatial autocorrelation is taken into account.

The Euro–Atlantic sector seems to be a hotspot for the solar influence on the troposphere. In fact, high positive correlations between solar activity and surface temperature in Europe have been reported in several papers (e.g. Tung and Camp, 2008; Lean and Rind, 2008; Lockwood et al., 2010; Woollings et al., 2010). We found a significant change in the mean late winter circulation over Europe, which results in important impacts on the near-surface climate. Figure 9 suggests that during solar minima more cold air is advected from the Arctic, thus resulting in colder winters for large parts of the continent. This configuration could be related to an increased frequency of blockings, which has been reported by Barriopedro et al. (2008). Some of the winters between 2005 and 2010, during a considerable long-lasting solar minimum, brought extreme cold spells over parts of Europe and it has already been suggested that the solar minimum may have played a role (Lockwood et al., 2010; Ineson et al., 2011). We showed that the average circulation pattern during those winters was the one expected in the condition of a low solar activity.

We could describe a similar solar signal by analysing SLP reconstructions reaching back to the 18th century, giving us further confidence on its temporal stability.

Unlike some authors, we did not find a significant correlation between the solar activity and the NAO, after analysing a 240-yr-long reconstruction of the NAO index. In such a long series, however, it was not possible to take into account the influence of the Quasi-Biennal Oscillation (QBO), which can modulate the interaction between the solar cycle and the polar vortex (Labitzke et al., 2006; Haigh and Roscoe, 2009; Cnossen and Lu, 2011). In any case, our conclusion does not contradict any of the earlier studies, which are based on shorter periods when the correlation between the NAO and the solar activity was indeed higher. In fact, after performing a running-correlation analysis, Thejll et al. (2003) had already pointed out that this correlation was highly variable over the last 130 yr, therefore very different results can arise by analysing only few decades. Moreover, we found that the correlation between solar activity and SLP over Europe

ACPD
12, 30371–30407, 2012

and the North Atlantic was much more variable for early winter than for late winter during the 20th century (not shown). A strong solar modulation of the NAO as described by Woollings et al. (2010) for DJF over the second half of the century is then probably a statistical artefact, because even a small change in the length of the analysed period would have lead to very different results.

We also found a significant relationship with the Eurasian index (representing the pressure see-saw between Western and Eastern Europe), an indication that the latter index is more linearly and steadily connected to the solar activity.

Our analysis shed some light on a possible weakening of the African branch of the sub-tropical jet during solar maxima. The reliability of upper-air data over North Africa however cannot be very high at the moment and further investigations are needed.

These results can help the ongoing efforts by the scientific community to describe a physical mechanism able to fully explain the observations. One of the main candidates is the "top-down" mechanism (see Sect. 4.2 of Gray et al., 2010, and references therein), which originates from the larger variability in the UV band, its impact on the temperatures in the stratosphere by means of changes in the ozone's production rates, and the coupling between the stratosphere and the troposphere. Ineson et al. (2011) and Chiodo et al. (2012) recently simulated this process using an ocean-atmosphere climate model, producing results which are very similar to those we found in the SLP reconstruction, although they used the standard DJF winter.

By comparing different data sets, we showed that the Twentieth Century Reanalysis (Compo et al., 2011) is also suitable for this kind of analysis, bearing in mind some limitations. In this sense, a thorough investigation of some apparent inhomogeneities and of their causes is necessary.

Future retrieval and digitisation of new historical upper-air data for the first part of the 20th century will further improve our understanding and estimation of the solar influence on the troposphere and will then facilitate the validation of the climate models, which remain fundamental for a full comprehension of the phenomenon.

ACPD
12, 30371–30407, 2012

Supplementary material related to this article is available online at: http://www.atmos-chem-phys-discuss.net/12/30371/2012/ acpd-12-30371-2012-supplement.zip.

Acknowledgements. This work was funded by the Swiss National Science Foundation through the Sinergia project FUPSOL and through NCCR Climate. We wish to thank ECMWF and the Royal Observatory of Belgium for providing ERA-40 data and the sunspot number, respectively. Support for the Twentieth Century Reanalysis Project dataset is provided by the US Department of Energy, Office of Science Innovative and Novel Computational Impact on Theory and Experiment (DOE INCITE) program, and Office of Biological and Environmental Research (BER), and by the National Oceanic and Atmospheric Administration Climate Program Office.

References

Allan, R. and Ansell, T.: A new globally complete monthly historical gridded mean sea level pressure dataset (HadSLP2): 1850–2004, J. Climate, 19, 5816–5842, doi:10.1175/JCLI3937.1, 2006.

Bal, S., Schimanke, S., Spangehl, T., and Cubasch, U.: On the robustness of the solar cycle signal in the Pacific region, Geophys. Res. Lett., 38, L14809, doi:10.1029/2011GL047964, 2011.

Barnston, A. G. and Livezey, R. E.: Classification, seasonality and persistence of low-frequency atmospheric circulation patterns, Mon. Weatnher Rev., 115, 1083–1126, 1987.

Barriopedro, D., García-Herrera, R., and Huth, R.: Solar modulation of Northern Hemisphere winter blocking, J. Geophys. Res., 113, D14118, doi:10.1029/2008JD009789, 2008.

Bengtsson, L., Hagemann, S., and Hodges, K. I.: Can climate trends be calculated from reanalysis data?, J. Geophys. Res., 109, D11111, doi:10.1029/2004JD004536, 2004.

Boberg, F. and Lundstedt, H.: Solar wind variations related to fluctuations of the North Atlantic Oscillation, Geophys. Res. Lett., 29, 1718, doi:10.1029/2002GL014903, 2002.

Boberg, F. and Lundstedt, H.: Solar wind electric field modulation of the NAO: a correlation analysis in the lower atmosphere, Geophys. Res. Lett., 30, 1825, doi:10.1029/2003GL017360, 2003.

Brönnimann, S., Ewen, T., Griesser, T., and Jenne, R.: Multidecadal signal of solar variability in the upper troposphere during the 20th century, Space Sci. Rev., 125, 305–317, doi:10.1007/s11214-006-9065-2, 2007a.
Brönnimann, S., Xoplaki, E., Casty, C., Pauling, A., and Luterbacher, J.: ENSO influence on Europe during the last centuries, Clim. Dynam., 28, 181–197, doi:10.1007/s00382-006-0175-z, 2007b.
Brönnimann, S., Grant, A. N., Compo, G. P., Ewen, T., Griesser, T., Fischer, A. M., Schraner, M., and Stickler, A.: A multi-data set comparison of the vertical structure of temperature variability and change over the Arctic during the past 100 years, Clim. Dynam., 39, 1577–1598, doi:10.1007/s00382-012-1291-6, 2012a.
Brönnimann, S., Griesser, T., and Stickler, A.: A gridded monthly upper-air data set from 1918 to 1957, Clim. Dynam., 38, 475–493, doi:10.1007/s00382-010-0940-x, 2012b.
Chiodo, G., Calvo, N., Marsh, D. R., and Garcia-Herrera, R.: The 11 year solar cycle signal in transient simulations from the whole atmosphere community climate model, J. Geophys. Res., 117, D06109, doi:10.1029/2011JD016393, 2012.
Cnossen, I. and Lu, H.: The vertical connection of the quasi-biennial oscillation-modulated 11 year solar cycle signature in geopotential height and planetary waves during Northern Hemisphere early winter, J. Geophys. Res., 116, D13101, doi:10.1029/2010JD015427, 2011.
Compo, G. P., Whitaker, J. S., Sardeshmukh, P. D., Matsui, N., Allan, R. J., Yin, X., Gleason, B. E., Vose, R. S., Rutledge, G., Bessemoulin, P., Brönnimann, S., Brunet, M., Crouthamel, R. I., Grant, A. N., Groisman, P. Y., Jones, P. D., Kruk, M. C., Kruger, A. C., Marshall, G. J., Maugeri, M., Mok, H. Y., Nordli, Ø., Ross, T. F., Trigo, R. M., Wang, X. L., Woodruff, S. D., and Worley, S. J.: The 20CR project, Q. J. Roy. Meteor. Soc., 137, 1–28, doi:10.1002/qj.776, 2011.
Crowley, T. J., Zielinski, G., Vinther, B., Udisti, R., Kreutz, K., Cole-Dai, J., and Castellano, E.: Volcanism and the little ice age, Pages News, 16, 22–23, 2008.
Eddy, J. A.: The Maunder minimum, Science, 192, 1189–1202, 1976.
Enfield, D. B., Mestas-Nuñez, A. M., and Trimble, P. J.: The Atlantic multidecadal oscillation and its relation to rainfall and river flows in the continental U.S., Geophys. Res. Lett., 28, 2077–2080, doi:10.1029/2000GL012745, 2001.
Fischer, A. M., Shindell, D. T., Winter, B., Bourqui, M. S., Faluvegi, G., Rozanov, E., Schraner, M., and Brönnimann, S.: Stratospheric winter climate response to ENSO in three

ACPD
12, 30371–30407, 2012

chemistry-climate models, Geophys. Res. Lett., 35, L13819, doi:10.1029/2008GL034289, 2008.
Frame, T. H. A. and Gray, L. J.: The 11-Yr Solar Cycle in ERA-40 Data: an update to 2008, J. Climate, 23, 2213–2222, doi:10.1175/2009JCLI3150.1, 2010.
Garny, H., Bodeker, G. E., and Dameris, M.: Trends and variability in stratospheric mixing: 1979–2005, Atmos. Chem. Phys., 7, 5611–5624, doi:10.5194/acp-7-5611-2007, 2007.
Gleisner, H., Thejill, P., Stendel, M., Kaas, E., and Machenhauer, B.: Solar signals in tropospheric re-analysis data: comparing NCEP/NCAR and ERA40, J. Atmos. Sol.-Terr. Phy., 67, 785–791, doi:10.1016/j.jastp.2005.02.001, 2005.
Graf, H. F. and Zanchettin, D.: Central Pacific El Niño, the “subtropical bridge” and eurasian climate, J. Geophys. Res., 117, D01102, doi:10.1029/2011JD016493, 2012.
Gray, L. J., Beer, J., Geller, M., Haigh, J. D., Lockwood, M., Matthes, K., Cubasch, U., Fleitmann, D., Harrison, G., Hood, L., Luterbacher, J., Meehl, G. A., Shindell, D., van Geel, B., and White, W.: Solar influences on climate, Rev. Geophys., 48, RG4001, doi:10.1029/2009RG000282, 2010.
Griesser, T., Brönnimann, S., Grant, A., Ewen, T., Stickler, A., and Comeaux, J.: Reconstruction of global monthly upper-level temperature and geopotential height fields back to 1880, J. Climate, 23, 5590–5609, doi:10.1175/2010JCLI3056.1, 2010.
Haigh, J. D.: The effects of solar variability on the Earth’s climate, Philos. T. R. Soc. Lond., 361, 95–111, doi:10.1098/rsta.2002.1111, 2003.
Haigh, J. D. and Roscoe, H. K.: The final warming date of the Antarctic polar vortex and influences on its interannual variability, J. Climate, 22, 5809–5819, doi:10.1175/2009JCLI2865.1, 2009.
Hansen, J., Ruedy, R., Glascoe, J., and Sato, M.: GISS analysis of surface temperature change, J. Geophys. Res., 104, 30997– 31022, 1999.
Harder, J. W., Fontenla, J. M., Pilewskie, P., Richard, E. C., and Woods, T. N.: Trends in solar spectral irradiance variability in the visible and infrared, Geophys. Res. Lett., 36, L07801, doi:10.1029/2008GL036797, 2009.
Ineson, S., Scaife, A. A., Knight, J. R., Manners, J. C., Dunstone, N. J., Gray, L. J., and Haigh, J. D.: Solar forcing of winter climate variability in the Northern Hemisphere, Nat. Geosci., 4, 753–757. doi:10.1038/NGEO1282, 2011.
Kalnay, E., Kanamitsu, M., Kistler, R., Collins, W., Deaven, D., Gandin, L., Iredell, M., Saha, S., White, G., Woollen, J., Zhu, Y., Chelliah, M., Ebisuzaki, W., Higgins, W.,

Janowiak, J., Mo, K., Ropelewski, C., Wang, J., Leetmaa, A., Reynolds, R., Jenne, R., and Joseph, D.: The NCEP/NCAR 40-year re-analysis project, B. Am. Meteorol. Soc., 77, 437–471, doi:10.1175/1520-0477(1996)077<0437:TNYRP>2.0.CO;2, 1996.

Kinter, J. L., Fennessy, M. J., Krishnamurthy, V., and Marx, L.: An evaluation of the apparent interdecadal shift in the tropical divergent circulation in the NCEP–NCAR Reanalysis, J. Climate, 17, 349–361, doi:10.1175/1520-0442(2004)017<0349:AEOTAI>2.0.CO;2, 2004.

Kistler, R., Kalnay, E., Collins, W., Saha, S., White, G., Woollen, J., Chelliah, M., Ebisuzaki, W., Kanamitsu, M., Kousky, V., van den Dool, H., Jenne, R., and Fiorino, M.: The NCEP-NCAR 50-year reanalysis: monthly means CD-ROM and documentation, B. Am. Meteorol. Soc., 82, 247–267, doi:10.1175/1520-0477(2001)082<0247:TNNYRM>2.3.CO;2, 2001.

Kodera, K.: Solar influence on the spatial structure of the NAO during the winter 1900–1999, Geophys. Res. Lett., 30, 1175, doi:10.1029/2002GL016584, 2003.

Labitzke, K., Kunze, M., and Brönnimann, S.: Sunspots, the QBO and the stratosphere in the north polar region – 20 years later, Meteorol. Z., 15, 355–363, doi:10.1127/0941-2948/2006/0136, 2006.

Lean, J. L. and Rind, D. H.: How natural and anthropogenic influences alter global and regional surface temperatures: 1889 to 2006, Geophys. Res. Lett., 35, L1870, doi:10.1029/2008GL034864, 2008.

Livezey, R. E. and Chen, W. Y.: Statistical field significance and its determination by Monte Carlo techniques, Mon. Weather Rev., 111, 46–59, 1983.

Lockwood, M.: Solar influence on global and regional climates, Surv. Geophys., 33, 503–534, doi:10.1007/s10712-012-9181-3, 2012.

Lockwood, M., Harrison, R. G., Woollings, T., and Solanki, S.: Are cold winters in Europe associated with low solar activity?, Environ. Res. Lett., 5, 024001, doi:10.1088/1748-9326/5/2/024001, 2010.

Luterbacher, J., Schmutz, C., Gyalistras, D., Xoplaki, E., and Wanner, H.: Reconstruction of monthly NAO and EU indices back to AD 1675, Geophys. Res. Lett., 26, 2745–2748, doi:10.1029/1999GL900576, 1999.

Luterbacher, J., Xoplaki, E., Dietrich, D., Jones, P. D., Davies, T. D., Portis, D., Gonzalez-Rouco, J. F., von Storch, H., Gyalistras, D., Casty, C., and Wanner, H.: Extending North Atlantic oscillation reconstructions back to 1500, Atmos. Sci. Lett., 2, 114–124, doi:10.1006/asle.2002.0047, 2001.

ACPD
12, 30371–30407, 2012

Luterbacher, J., Xoplaki, E., Dietrich, D., Rickli, R., Jacobeit, J., Beck, C., Gyalistras, D., Schmutz, C., and Wanner, H.: Reconstruction of sea level pressure fields over the Eastern North Atlantic and Europe back to 1500, Clim. Dynam., 18, 545–561, doi:10.1007/S00382-001-0196-6, 2002.

Martin-Puertas, C., Matthes, K., Brauer, A., Muscheler, R., Hansen, F., Petrick, C., Aldahan, A., Possnert, G., van Geel, B.: Regional atmospheric circulation shifts induced by a grand solar minimum, Nat. Geosci., 5, 397–401, doi:10.1038/ngeo1460, 2012.

Moron, V. and Plaut, G.: The impact of El Niño–southern oscillation upon weather regimes over Europe and the North Atlantic during boreal winter, Int. J. Climatol., 23, 363–379, doi:10.1002/joc.890, 2003.

Peixoto, J. P. and Oort, A. H.: Observed mean state of the atmosphere, in: Physics of Climate, Springer-Verlag, New York, USA, 131–175, 1992.

Rayner, N. A., Parker, D. E., Horton, E. B., Folland, C. K., Alexander, L. V., Rowell, D. P., Kent, E. C., and Kaplan, A.: Global analyses of sea surface temperature, sea ice, and night marine air temperature since the late nineteenth century, J. Geophys. Res., 108, 4407, doi:10.1029/2002JD002670, 2003.

Rayner, N. A., Brohan, P., Parker, D. E., Folland, C. K., Kennedy, J. J., Vanicek, M., Ansell, T. J., and Tett, S. F. B.: Improved analyses of changes and uncertainties in sea surface temperature measured in situ since the mid-nineteenth century: the HadSST2 dataset, J. Climate, 19, 446–469, doi:10.1175/JCLI3637.1, 2006.

Roy, I. and Haigh, J. D.: Solar cycle signals in sea level pressure and sea surface temperature, Atmos. Chem. Phys., 10, 3147–3153, doi:10.5194/acp-10-3147-2010, 2010.

Roy, I. and Haigh, J. D.: The influence of solar variability and the quasi-biennial oscillation on lower atmospheric temperatures and sea level pressure, Atmos. Chem. Phys., 11, 11679–11687, doi:10.5194/acp-11-11679-2011, 2011.

Russell, C. T., Luhmann, J. G., and Jian, L. K.: How unprecedented a solar minimum?, Rev. Geophys., 48, RG2004, doi:10.1029/2009RG000316, 2010.

Schmutz, C. and Wanner, H.: Low frequency variability of atmospheric circulation over Europe between 1785 and 1994, Erdkunde, 52, 81–94, 1998.

Schrijver, C. J., Livingston, W. C., Woods, T. N., and Mewaldt, R. A.: The minimal solar activity in 2008–2009 and its implications for long-term climate modelling, Geophys. Res. Lett., 38, L06701, doi:10.1029/2011GL046658, 2011.

Shapiro, A. I., Schmutz, W., Rozanov, E., Schoell, M., Haberreiter, M., Shapiro, A. V., and Nyeki, S.: A new approach to the long-term reconstruction of the solar irradiance leads to large historical solar forcing, Astron. Astrophys., 529, A67, doi:10.1051/0004-6361/201016173, 2011.

Shindell, D. T., Rind, D., Balachandran, N. K., Lean, J., and Lonergan, P.: Solar cycle variability, ozone, and climate, Science, 284, 305–308, doi:10.1126/science.284.5412.305, 1999.

Shindell, D. T., Schmidt, G. A., Mann, M. E., Rind, D., and Waple, A.: Solar forcing of regional climate change during the Maunder Minimum, Science, 294, 2149–2152, doi:10.1126/science.1064363, 2001.

Stickler, A., Grant, A. N., Ewen, T., Ross, T. F., Vose, R. S., Comeaux, J., Bessemoulin, P., Jylhä, K., Adam, W. K., Jeannet, P., Nagurny, A., Sterin, A. M., Allan, R., Compo, G. P., Griesser, T., and Brönnimann, S.: The comprehensive historical upper-air network, B. Am. Meteorol. Soc., 91, 741–751, doi:10.1175/2009BAMS2852.1, 2010.

Thejll, P., Christiansen, B., and Gleisner, H.: On correlations between the North Atlantic oscillation, geopotential heights, and geomagnetic activity, Geophys. Res. Lett., 30, 1347, doi:10.1029/2002GL016598, 2003.

Thompson, D. W. J., Kennedy, J. J, Wallace, J. M., and Jones, P. D.: A large discontinuity in the mid-twentieth century in observed global-mean surface temperature, Nature, 453, 646–649, doi:10.1038/nature06982, 2008.

Tinsley, B. A. and Yu, F.: Atmospheric ionization and clouds as links between solar activity and climate, in: Solar Variability and its Effects on Climate, Geophysical Monograph, vol. 141, AGU Press, Washington, DC, 321–339, 2004.

Tung, K. K. and Camp, C. D.: Solar cycle warming at the Earth's surface in NCEP and ERA-40 data: a linear discriminant analysis, J. Geophys. Res., 113, D05114, doi:10.1029/2007JD009164, 2008.

Uppala, S. M., Kållberg, P. W., Simmons, A. J., Andrae, U., da Costa Bechtold, V., Fiorino, M., Gibson, J. K., Haseler, J., Hernandez, A., Kelly, G. A., Li, X., Onogi, K., Saarinen, S., Sokka, N., Allan, R. P., Andersson, E., Arpe, K., Balmaseda, M. A., Beljaars, A. C. M., van de Berg, L., Bidlot, J., Bormann, N., Caires, S., Chevallier, F., Dethof, A., Dragosavac, M., Fisher, M., Fuentes, M., Hagemann, S., Hólm, E., Hoskins, B. J., Isaksen, L., Janssen, P. A. E. M., Jenne, R., McNally, A. P., Mahfouf, J.-F., Morcrette, J.-J., Rayner, N. A., Saunders, R. W., Simon, P., Sterl, A., Trenberth, K. E., Untch, A., Vasiljevic, D., Viterbo, P., and Woollen, J.: The ERA-40 re-analysis, Q. J. Roy. Meteor. Soc., 131, 2961–3012, doi:10.1256/qj.04.176, 2005.

van Loon, H., Meehl, G. A., and Shea, D. J.: Coupled air-sea response to solar forcing in the Pacific region during northern winter, J. Geophys. Res., 112, D02108, doi:10.1029/2006JD007378, 2007.

Woollings, T., Lockwood, M., Masato, G., Bell, C., and Gray, L.: Enhanced signature of solar variability in Eurasian winter climate, Geophys. Res. Lett., 37, L20805, doi:10.1029/2010GL044601, 2010.

Zanchettin, D., Bothe, O., Graf, H.-F., Luterbacher, J., Jungclaus, J. H., and Timmreck, C.: Background conditions influence decadal climate response to strong volcanic eruptions, in review, J. Geophys. Res., 2012a.

Zanchettin, D., Timmreck, C., Bothe, O., Lorenz, S., Hegerl, G., Graf, H.-F., Luterbacher, J., and Jungclaus, J. H.: Delayed winter warming: a decadal dynamical response to strong tropical volcanic eruptions, in review, Geophys. Res. Lett., 2012b.

Table 1. Differences between solar maximum and minimum composites for various atmospheric indices in JFM over the period 1749–1990, together with their 99 % confidence intervals. Values in bold are significantly different from zero at 5 % level after a two-sided Student's t-test for the differences (note that none of the indices is subject to a significant serial correlation when using JFM averages). Refer to the text for details about the filtering procedure.

	Filtered	Unfiltered
NAO1	0.38 ± 0.54	0.26 ± 0.43
NAO2	0.34 ± 0.58	0.23 ± 0.46
EU1	$\mathbf{-0.38 \pm 0.30}$	$\mathbf{-0.21 \pm 0.24}$
EU2	$\mathbf{-0.42 \pm 0.39}$	$\mathbf{-0.29 \pm 0.31}$

ACPD
12, 30371–30407, 2012

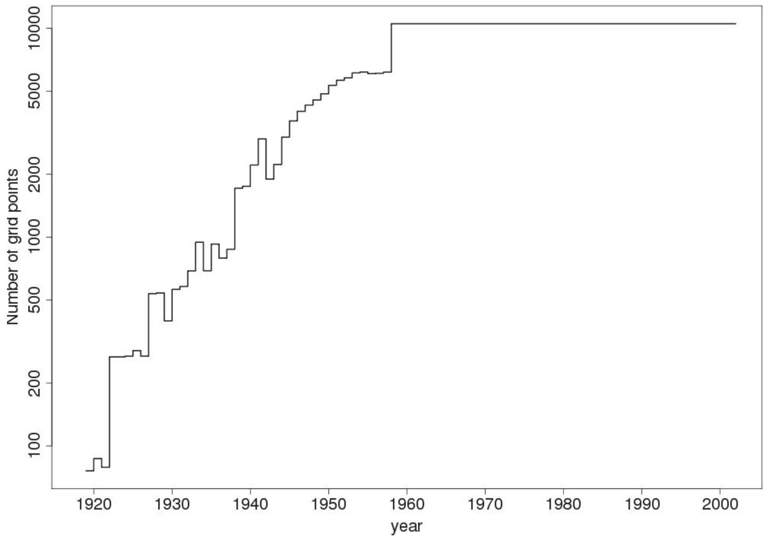

Fig. 1. Evolution of the number of available grid points in REC2 (JFM). Note that the scale is logarithmic.

ACPD
12, 30371–30407, 2012

Influence of the sunspot cycle on the Northern Hemisphere wintertime circulation

Y. Brugnara et al.

Title Page
Abstract | Introduction
Conclusions | References
Tables | Figures
Back | Close
Full Screen / Esc
Printer-friendly Version
Interactive Discussion

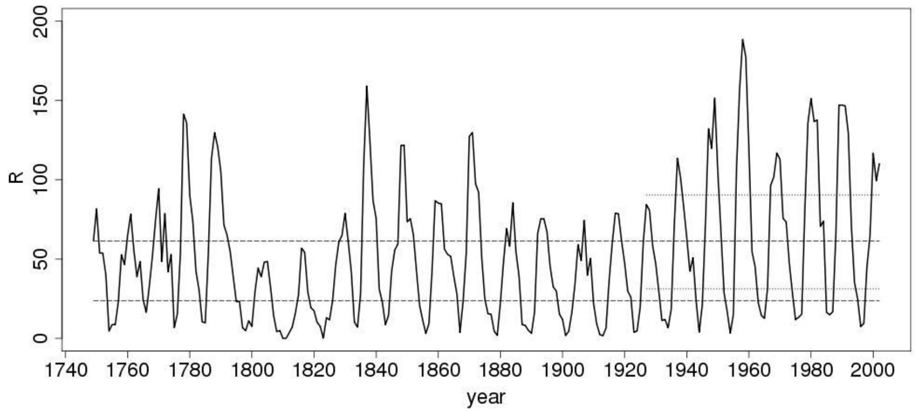

Fig. 2. Evolution of the seasonally-averaged International Sunspot Number (R) in JFM over the analysed period (1749–2002). The dashed (dotted) lines mark the thresholds used to define the composites for the surface (upper-air) analysis.

ACPD
12, 30371–30407, 2012

Influence of the sunspot cycle on the Northern Hemisphere wintertime circulation

Y. Brugnara et al.

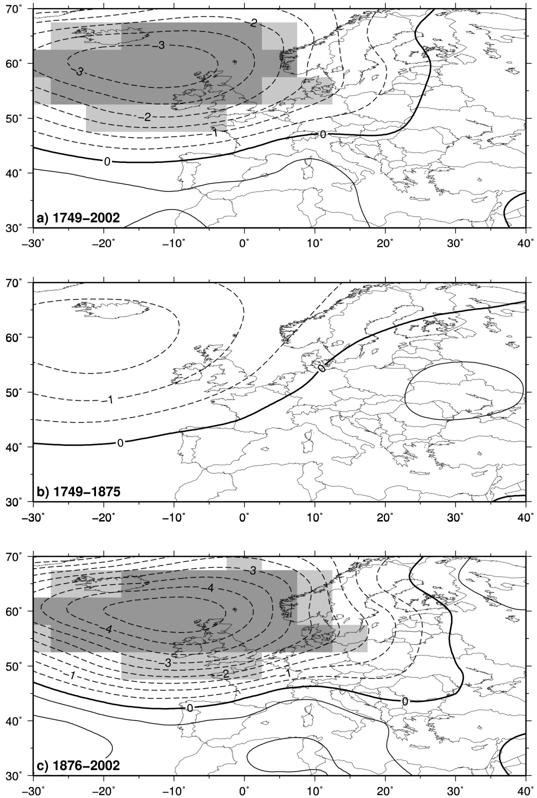

Fig. 3. Maps of differences between maxima and minima composites for the SLP reconstruction by Luterbacher et al. (2002) over **(a)** the whole analysed period, **(b)** and **(c)** the first and the second half of the whole period respectively. Light (dark) gray shaded areas indicate significant differences at the 5 % (1 %) level after a Student's t-test, units are hPa.

ACPD
12, 30371–30407, 2012

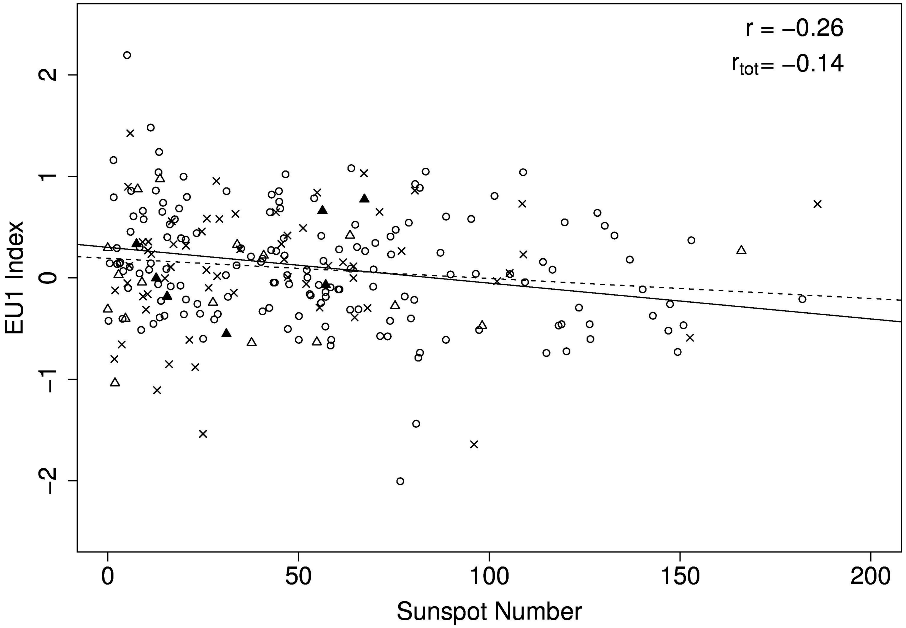

Fig. 4. Scatter plot of the Sunspot Number versus the EU1 index reconstructed by Luterbacher et al. (1999), both are seasonal (JFM) mean over the period 1749–1990. Triangles represent volcanic years, while crosses represent ENSO years; filled triangles are both volcanic and ENSO years. The dashed line is the least squares regression line considering every data point, while the continuous line is for "neutral" years only (no volcanic and no ENSO years); the respective Pearson's coefficients r_{tot} and r are also shown.

ACPD
12, 30371–30407, 2012

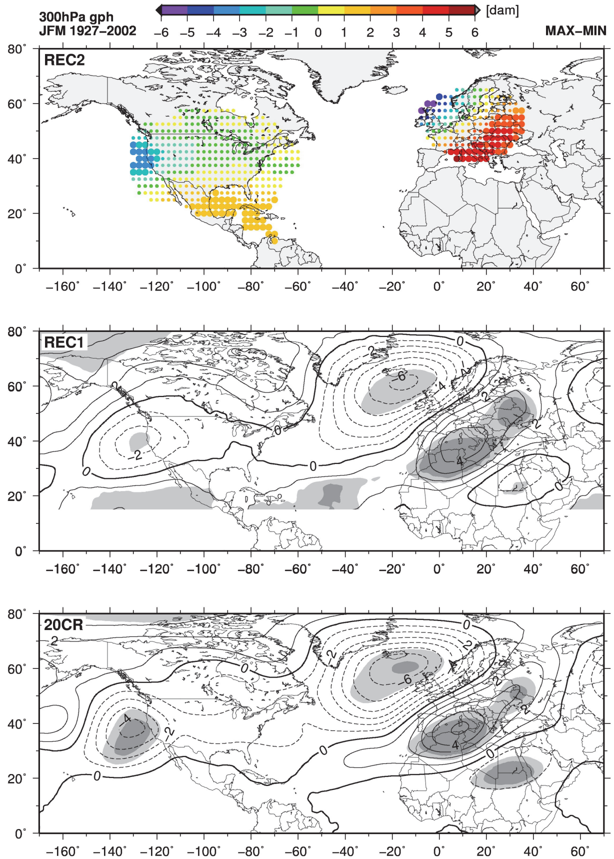

Fig. 5. Maps of differences between maxima and minima composites for 300 hPa geopotential height in the REC2 reconstruction (top panel, big circles represent significant differences at 5 % level after a Student's *t*-test), the REC1 reconstruction (middle panel) and the 20CR (bottom panel). Shadings as in Fig. 3, units are dam.

ACPD
12, 30371–30407, 2012

Influence of the sunspot cycle on the Northern Hemisphere wintertime circulation

Y. Brugnara et al.

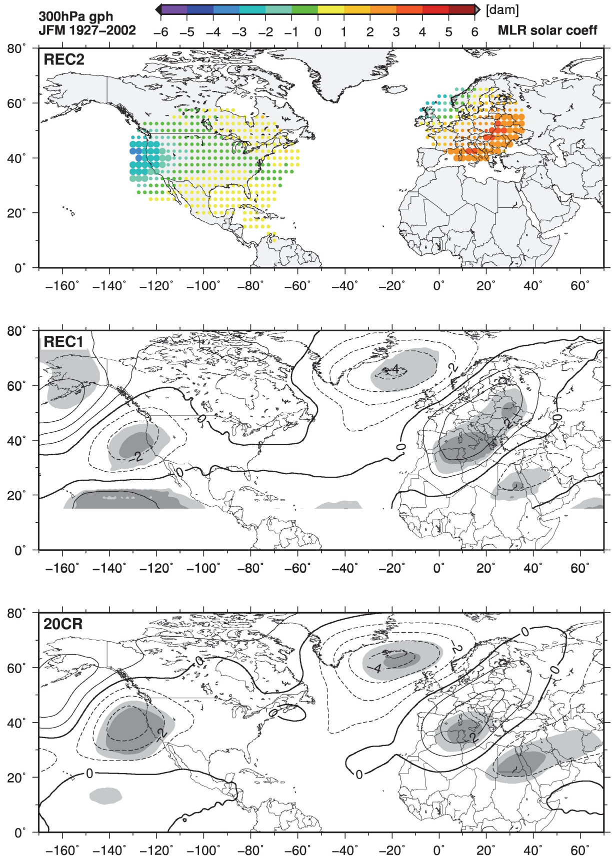

Fig. 6. Same as Fig. 5, but showing the MLR solar coefficient (in dam/100 units of *R*) instead of the composites difference.

ACPD
12, 30371–30407, 2012

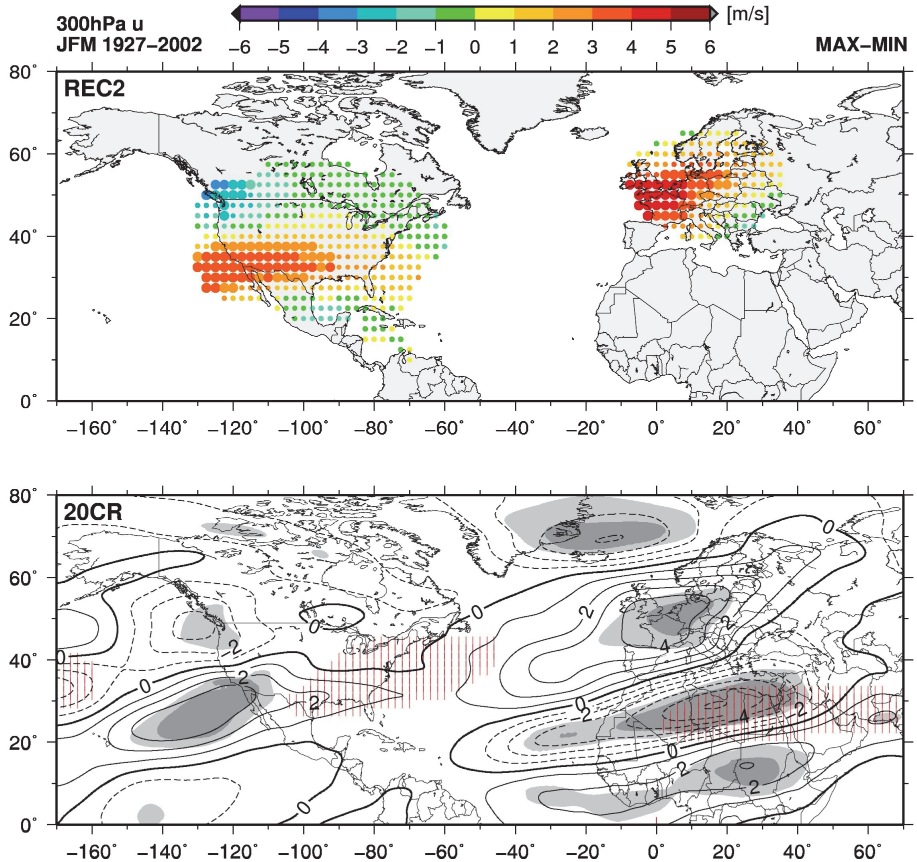

Fig. 7. Similar to Fig. 5, but showing zonal wind in $m\,s^{-1}$. Red lines localise the strongest sections of the jet-stream ($\geq 30\,m\,s^{-1}$) in the 1927–2002 climatology for 20CR.

ACPD
12, 30371–30407, 2012

Influence of the sunspot cycle on the Northern Hemisphere wintertime circulation

Y. Brugnara et al.

Title Page
Abstract | Introduction
Conclusions | References
Tables | Figures
◂I | ▸I
◂ | ▸
Back | Close
Full Screen / Esc
Printer-friendly Version
Interactive Discussion

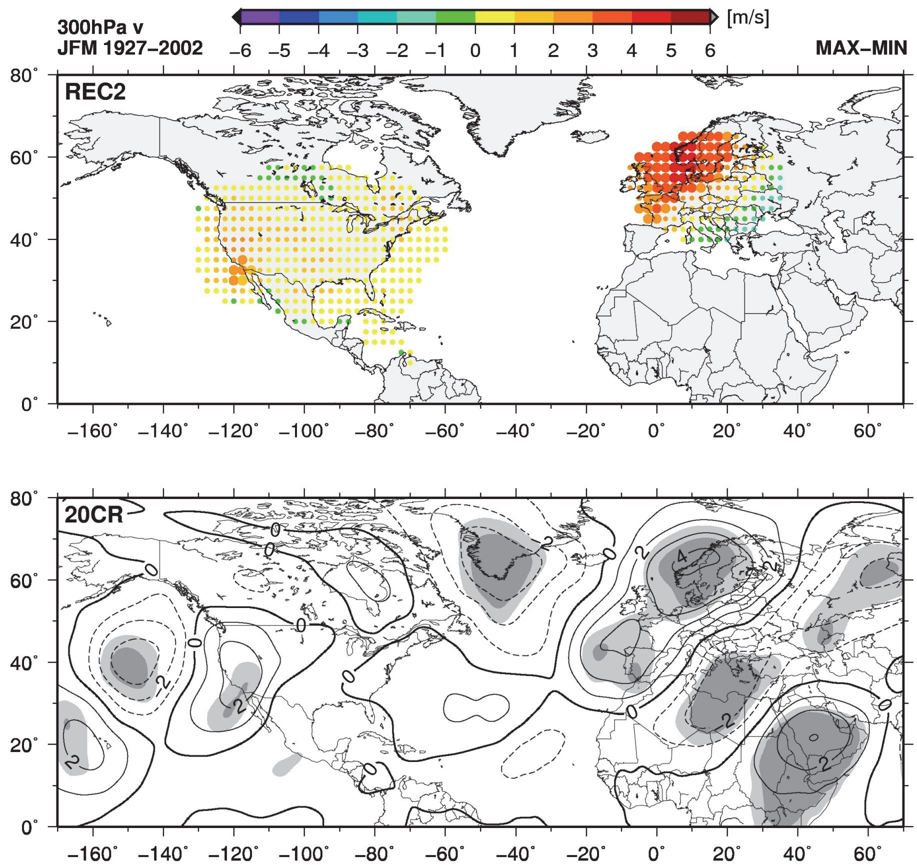

Fig. 8. Similar to Fig. 5, but showing meridional wind in m s^{-1}.

ACPD
12, 30371–30407, 2012

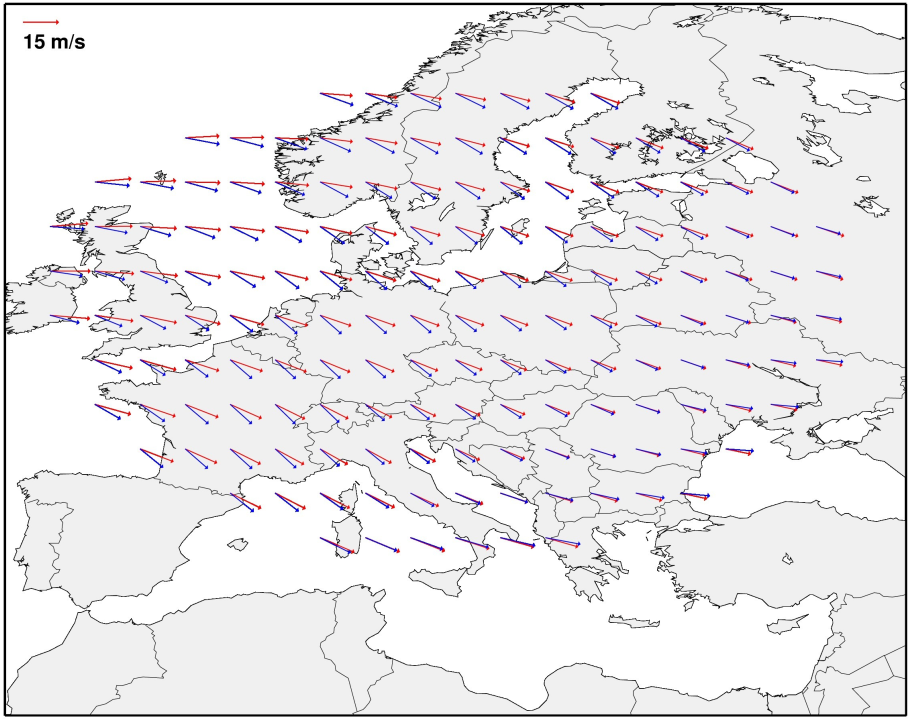

Fig. 9. Wind vectors representing average conditions at 300 hPa in JFM during solar maxima (red arrows) and solar minima (blue arrows) over Europe. The length of the arrows is linearly proportional to the wind speed. Data are from REC2 (1927–2002).

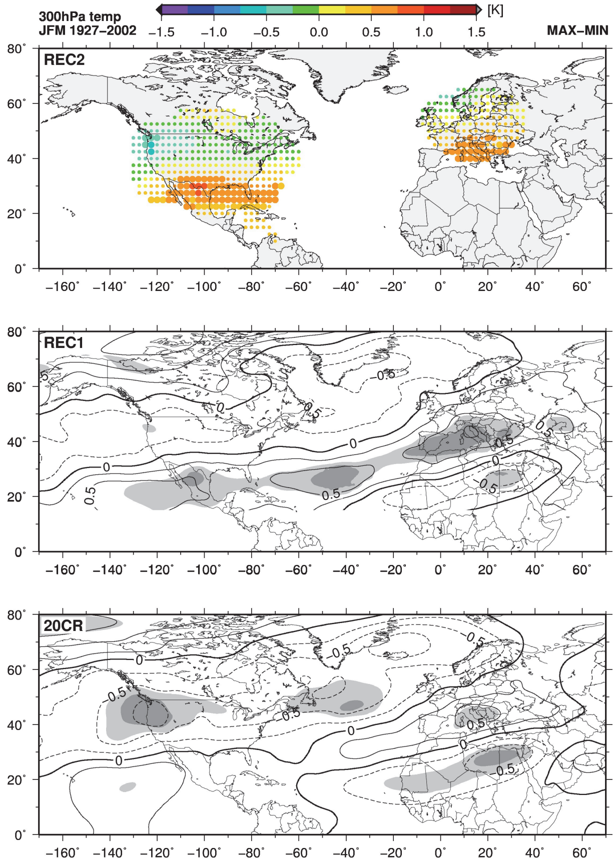

Fig. 10. Similar to Fig. 5, but showing temperature in K.

ACPD
12, 30371–30407, 2012

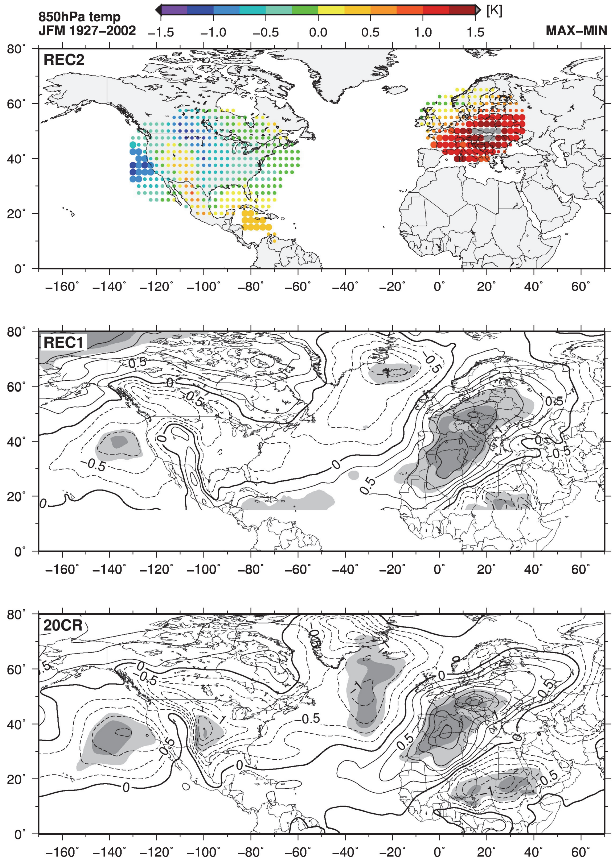

Fig. 11. Same as Fig. 10, but for 850 hPa.

ACPD
12, 30371–30407, 2012

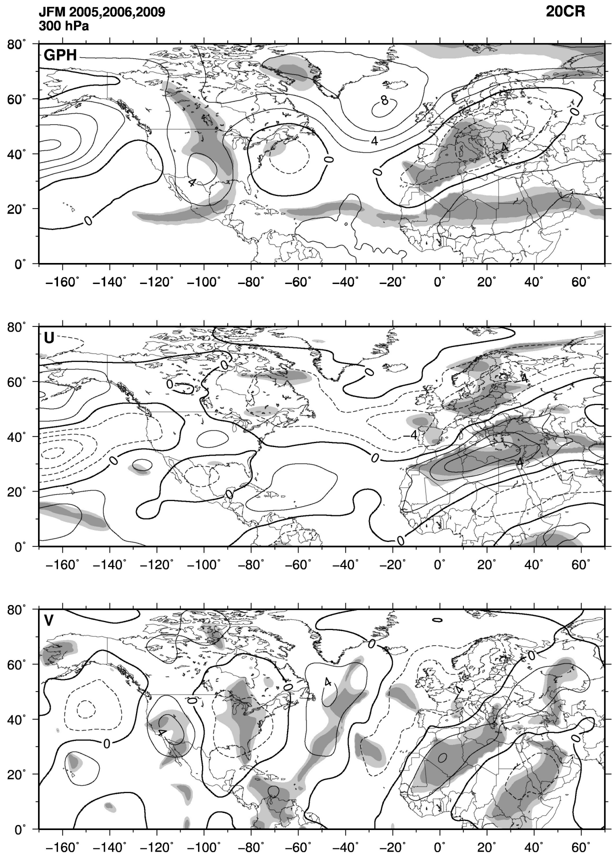

Fig. 12. Average anomalies in JFM during the years 2005, 2006 and 2009 in 20CR for geopotential height (top panel, in dam), zonal wind (middle panel, in $m\,s^{-1}$) and meridional wind (bottom panel, in $m\,s^{-1}$). Shadings represent statistical significance like in the previous figures.

ACPD
12, 30371–30407, 2012

Influence of the sunspot cycle on the Northern Hemisphere wintertime circulation

Y. Brugnara et al.